Particuology 17 (2014) 92–96

Contents lists available at ScienceDirect

Particuology

journal homepage: www.elsevier.com/locate/partic

# Attritor-milling of poly(amide imide) suspensions

M.F.H. Wolff[a,*], S. Antonyuk[a], S. Heinrich[a], G.A. Schneider[b]

[a] Hamburg University of Technology, Institute of Solids Process Engineering and Particle Technology, Denickestr. 15, 21073 Hamburg, Germany
[b] Hamburg University of Technology, Institute of Advanced Ceramics, Denickestr. 15, 21073 Hamburg, Germany

ARTICLE INFO

*Article history:*
Received 4 September 2013
Received in revised form 28 October 2013
Accepted 23 November 2013

*Keywords:*
Attritor
Polymer
Grinding
Suspension

ABSTRACT

The milling behavior of poly(amide imide), which serves as a prototypical hydrophilic high-performance polymer with a high glass transition temperature, was investigated. Various milling conditions (milling times up to 7 h, stirrer tip speeds of 3.4–4.9 m/s, and mass concentrations of 5–20%) were tested, and particle sizes as low as $d_{50,3} \sim 3$ μm were obtained. The milling was performed at 11 °C in an attritor. Differential scanning calorimetry and thermogravimetric analysis were performed before and after milling to investigate the effect of milling on the glass transition temperature and on the decomposition behavior of the polymer. The suspension obtained after milling was observed to be stable without the addition of stabilizers or the adjustment of the pH value, and no negative effect of milling on the polymer properties was observed. The attritor technique proved to be an adequate and efficient milling tool for the production of micrometer-sized high-performance polymer suspensions.



## 1. Introduction

Polymer nanoparticles and nanocomposites are of great interest for the manufacturing of nano- and microstructured materials and have been studied extensively throughout the past several years. However, in contrast to ceramic particles, relatively little is known about the milling behavior of polymer particles in stirred media mills. In stirred media milling, mechanical stresses, which are generated by collision with milling balls, act on the milling media and cause them to break into smaller pieces. It is an important process for producing micrometer- and nanometer-sized powder particles, which can be used in various ways, for example, as fillers and pigments, or in shape-forming processes for component fabrication (Kwade, 1999; Sommer, Stenger, Peukert, & Wagner, 2006; Stenger, Mende, Schwedes, & Peukert, 2005).

In this study, we investigated the milling behavior of poly(amide imide) (PAI). PAI is a thermoplast with generally very good mechanical and thermal properties. Due to high intermolecular interaction and high intramolecular chain stiffness, PAI is one of the strongest and stiffest of all polymers. In particular, unlike most other high-performance polymers, PAI exhibits very good adhesion to hydrophilic surfaces and is therefore very promising as, for example, a coating polymer for ceramics used in various applications. However, PAI is chemically rather resistant, and therefore, no solvents for the polymer with desirable properties (nontoxic, intermediate vapor pressure) exist.

Stirred media milling of ceramic particles is well analyzed and described in the literature (Breitung-Faes & Kwade, 2008; Essl, Janssen, & Claussen, 1999; Knieke et al., 2010; Kwade & Schwedes, 2002; Kwade, 1999), with a focus on the sub-micrometer and nanometer scales (Mende, Stenger, Peukert, & Schwedes, 2003; Stenger et al., 2005). It has been observed that when ground particles in a suspension reach the micrometer and sub-micrometer-scale, particle–particle interactions typically become dominant. These interactions can lead to the (re)agglomeration of the ground particles, and no further size reduction occurs (Knieke, Sommer, & Peukert, 2009; Mende et al., 2003). Some important investigations have shown, for example, that milling ball size has a pronounced effect on the milling results (Mankosa, Adel, & Yoon, 1986; Mende et al., 2003) and that, on the other hand, the milling tip speed is of less importance (Mende et al., 2003). Kwade and co-workers (Blecher, Kwade, & Schwedes, 1996; Kwade, Blecher, & Schwedes, 1996; Mankosa et al., 1986) measured the stress parameters (stress number, stress energy, and specific energy) in stirred mills for limestone and developed a general approach for describing the milling behavior of particles larger than approximately 1 μm. Stenger et al. (2005) studied the applicability of this approach to the sub-micrometer and nanometer size range and observed that mean diameters of less than 10 nm can be reached for alumina. Sommer et al. (2006) studied the agglomeration and breakage of nanoparticles in stirred media mills by applying a population balance model. An alternative technique to stirred media milling is

* Corresponding author. Tel.: +49 40428782811.
*E-mail address:* michael.wolff@tuhh.de (M.F.H. Wolff).

1674-2001 
http://dx.doi.org/10.1016/j.partic.2013.11.005

jet milling, which is used for many different materials, including ceramics, pharmaceuticals, and polymers (Nykamp, Carstensen, & Muller, 2002), but is more complex with respect to material handling.

An important parameter that is often used to describe the milling process is the stress intensity *SI*GM

$$SI_{GM} = \frac{d_{GM}^3 \rho_{GM} v_t^2}{m_{GM}}, \quad (1)$$

where $d_{GM}$, $m_{GM}$, and $\rho_{GM}$ are the diameter, mass, and density of a milling ball, respectively, and $v_t$ describes the tip speed of the stirrer. As indicated by Schmidt, Plata, Troeger, and Peukert (2012), the milling theory for ceramics must be modified for polymers to include the different mechanisms of stress transformation in polymers, i.e., inelastic deformation (ultimately resulting in thermal energy) instead of the creation of new fracture surfaces. The critical diameter $\delta_c$ for which the stress state in a ductile material will no longer lead to new surfaces, but exclusively to inelastic deformation, is given by the ratio of the energy release rate (toughness) *G*Ic (J/m$^2$), which is the energy necessary to increase the crack area by a unit area (Munz & Fett, 2001), to the yield strength $\sigma_Y$ (Dugdale, 1960):

$$\delta_c = \frac{K_{Ic}^2}{2\sigma_Y E} = \frac{G_{Ic}}{2\sigma_Y(1-\nu^2)}, \quad (2)$$

where $\nu$ is the Poisson's ratio and *K*Ic (MPa m$^{1/2}$) the fracture toughness.

Eq. (2) describes the size of the plastic zone at the crack front, within which the stress everywhere is given by the yield stress $\sigma_Y$ and no crack propagation can take place.

Although many investigations have been carried out on inorganic materials, hardly any studies have focused on the wet-milling behavior of high-performance polymers, such as poly(ether sulfone), poly(ether ether ketone), or poly(amide imide). Because polymers exhibit higher ductility and lower strength than ceramics, the milling behaviors of polymers and ceramics are different, and it is not clear what final particle sizes are feasible. Recently, Schmidt et al. (2012) investigated the milling behavior of polymers poly(styrene) (PP) and poly(ether ether ketone) (PEEK) for the first time. The authors used a stirred media mill operating at temperatures as low as −80 °C, ball sizes of 0.7 mm, and milling times as long as 29.5 h and obtained particle sizes of $d_{50,3} \sim 1.9$ μm for PP and $d_{50,3} \sim 2.8$ μm for PEEK. When milling at room temperature, the obtained particle sizes were 3.3 μm for PP and 7.3 μm for PEEK, which suggests that the dependence on temperature was surprisingly small. In general, the milling properties of a powder mainly depend on the primary particle size, the strength, and ductility. This behavior sets special demands on the milling of polymers because they are ductile and tend to absorb impact energy, thereby heating up instead of creating fracture surfaces. Therefore, high impact energies and suspension cooling are typically required. It is known that near the glass transition temperature ($T_g$) of a polymer, the polymer's ductility increases very strongly with temperature and the material becomes rubberlike, which indicates that the milling temperature must be kept far below $T_g$ throughout the milling process. An important parameter is the difference between the glass transition and milling temperature $Tg - Tgrinding$. Therefore, high-performance polymers, which typically have $T_g > 250$ °C, are better suited for milling than some elastomers, which have a $T_g$ below room temperature.

## 2. Materials and methods

### 2.1. Materials

The seed powder used in this study was the poly(amide imide) powder Torlon® 4000TF poly(amide imide), with a median diameter $d_{50,3} = 22$ μm and purity ≥ 99%, kindly provided by Solvay Specialty Polymers Germany GmbH. According to the manufacturer, the material has a Rockwell hardness (E-scale) of ∼86, a fracture strain of ∼7.6%, and a glass transition temperature in the range of $T_g \sim 275$–280 °C. The tensile modulus of elasticity is approximately $E \sim 5.2$ GPa (Becker, Bottenbruch, & Braun, 1994; Mark, 1999). The literature values for the yield stress $\sigma_Y$ are not uniform and vary between 117 and 189 MPa (e.g., Mark, 1999). The mechanical properties depend quite strongly on the processing conditions and post-molding annealing. The critical energy release rate or toughness *G*Ic is given by the manufacturer as $G_{Ic} \sim 3.4$ kJ/m$^2$.

The grinding balls were composed of yttria-stabilized zirconia (YSZ, $\rho_{YSZ} = 6.0$ g/cm$^3$, 3-mm and 0.5-mm ball sizes) and α-alumina (α-$Al_2O_3$, $\rho_{Al_2O_3} = 3.95$ g/cm$^3$, 1-mm ball size).

### 2.2. Experimental setup

The milling was carried out in an attritor (model PE 075, Netsch-Feinmahltechnik GmbH). The instrument consisted of a vertically arranged vessel with a volumetric capacity of 750 mL. The seed powder was first suspended in 100 mL of deionized water and poured into the vessel. The milling balls (1.5 kg for YSZ and 0.9 kg for α-$Al_2O_3$) were then added, and the vessel was filled with another 100 mL of water. The attritor was cooled to a constant temperature of 11 °C, which indicates that the milling was carried out approximately $|T_{grinding} - T_G| \sim 270$ °C below the glass transition.

Particle size analysis was carried out via static light scattering (SLS) (Beckman Coulter LS13320, Beckman Coulter Inc.). Specimens for particle size analysis were prepared by pipetting a few mL of the suspensions at low attritor speeds. Mie theory was used to calculate the size distribution. The real part of the refractive index was taken from Bryce et al. (2004) to be 1.65 for the laser wavelength used ($\lambda = 750$ nm). The imaginary part of the refractive index, which is not reported in the literature for this material, was estimated to be 0.05, which is a typical value for a non-transparent polymer. The obscuration level was set to approximately 8% for all measurements. Each measurement lasted 60 s and was repeated three times.

The zeta potential was measured with an electroacoustic spectrometer (DT-1202, Quantachrome) at a pH value of 4.5 (mass concentration 2%). Scanning electron microscopy (SEM) was carried out with a Leo Gemini 1530 at 5 keV. Differential scanning calorimetry (DSC) was performed using a Netsch DSC 204 F1 Phoenix at a heating rate of 10 K/min. Thermogravimetric analysis (TGA) was performed with a Q500 TA Instruments (USA).

## 3. Results and discussion

### 3.1. Morphological characterization

To gain insight into the particle shape and structure before and after milling, scanning electron microscopy was used. Fig. 1 shows micrographs of the dry powder before milling (Fig. 1(a)), of the suspended polymer pipetted from the milling suspension immediately before the beginning of the milling process (Fig. 1(b)), and of the suspension after milling for 7 h with 0.5-mm milling balls (Fig. 1(c) and (d)). The rough surface shown in the background exists because

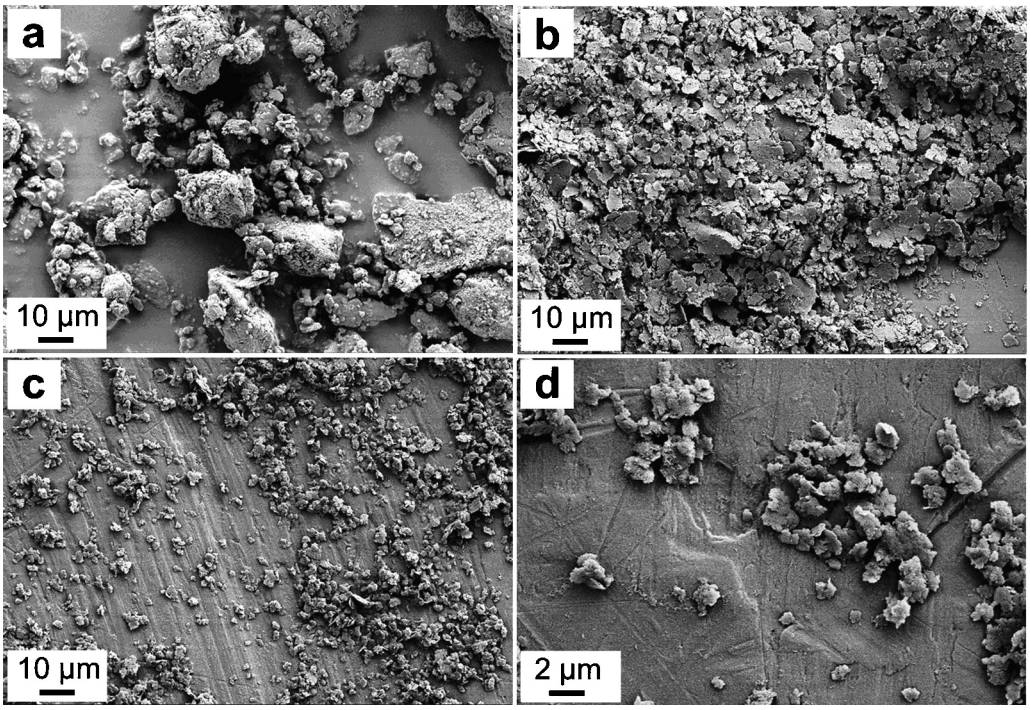


**Fig. 1.** SEM images of the dry Torlon® 4000 TF poly(amide imide) before milling (a), of the suspended polymer before milling (b), and of the polymer suspension after milling (c, d).

the suspension was placed directly on the metal holder to prevent the particles from into the polymer foil. To obtain mostly isolated particles for microscopy, the suspensions were diluted in deionized water and then a droplet was placed onto the metal plates.

Before grinding, the particles appeared slightly agglomerated, but the primary particle size is clearly larger than that of the particles after milling, which indicates that the milling process was at least partially a true milling process and not a pure deagglomeration process.

### 3.2. Influence of stirrer tip speed, mass concentration, and milling time

In Fig. 2(a), particle size distribution is plotted for the unground powder (suspended in $H_2O$) and for the three stirrer tip speeds that were tested. As shown, only a small effect of this speed on the particle size distribution was observed. The effect of the milling time on the particle size distribution for three different mass concentrations of the particle suspension (5%, 10%, and 20%) and 1-mm $Al_2O_3$ milling balls is shown in Fig. 2(c). As is known to occur for inorganic materials, a roughly exponential decay can be observed, and interestingly, the highest mass load of 20% yielded the best milling result. The improved milling result for mass loads also suggests that stress events between feed particles contribute to the milling process. If only stress events between milling balls and feed particles are considered, the milling process should be enhanced by an increase in feed particle number. Fig. 2(b) shows the volume-related cumulative particle size distribution of the polymer for several milling times. For $t = 0$ h (initial suspension) and $t = 7$ h (maximum milling time), the measurement was repeated many times for various suspensions. Although the initial particle size distribution is rather narrowly distributed, there is a considerable spread in the distribution for the final suspension after 7 h of milling. The deviation of the spherical shape of the milled particles, as observed in the SEM images (Fig. 1), leads to a slightly larger error in the measurement of the particle size distribution.

### 3.3. Stability of polymer suspension

Particle size measurements after 1, 7, and 30 d of storage yielded basically no change in the particle size distribution compared to the results obtained immediately after milling, which means that the polymer suspensions were stable after milling and that reagglomeration of the milled particles was avoided. The good stability of the suspension is in accordance with the measured value of the zeta potential, $\zeta \approx -30$ mV, which is a rather large magnitude for a polymer solution and indicates that surface charges are present, which lead to a repulsion of polymer particles. Sedimentation of the particles in the suspension occurred over longer storage times (several hours), but slight manual agitation of the suspension sufficed to resuspend the particles.

In addition to the suspension stability, the thermal stability was analyzed by DSC and TGA (Fig. 3). This analysis was performed for the as-received powder to determine its decomposition behavior and glass transition temperature and for a sample milled for 7 h with 0.5-mm milling balls to detect any change in $T_g$ and decomposition behavior that might be caused by the milling. The DSC yielded a glass transition within the range of 263 and 269 °C for the as-received polymer powder before milling and a slightly higher range of 267 and 277 °C after 7 h of milling. It can be concluded that the measured $T_g$ is within the range of literature values for the glass transition of this polymer, and no reduction in $T_g$ was caused by the milling. Thermogravimetric analysis, which was carried out at a heating rate of $T = 5$ K/min in synthetic air, indicated that decomposition begins at approximately $T = 350$ °C and is completed at approximately $T = 630$ °C. The milled sample exhibits a slightly increased decomposition rate of approximately 500 °C up to a content of 80 wt%, which is then followed by a slightly higher resistance to degradation compared to that of the as-received powder. TGA analysis also verified that no substantial amount of milling

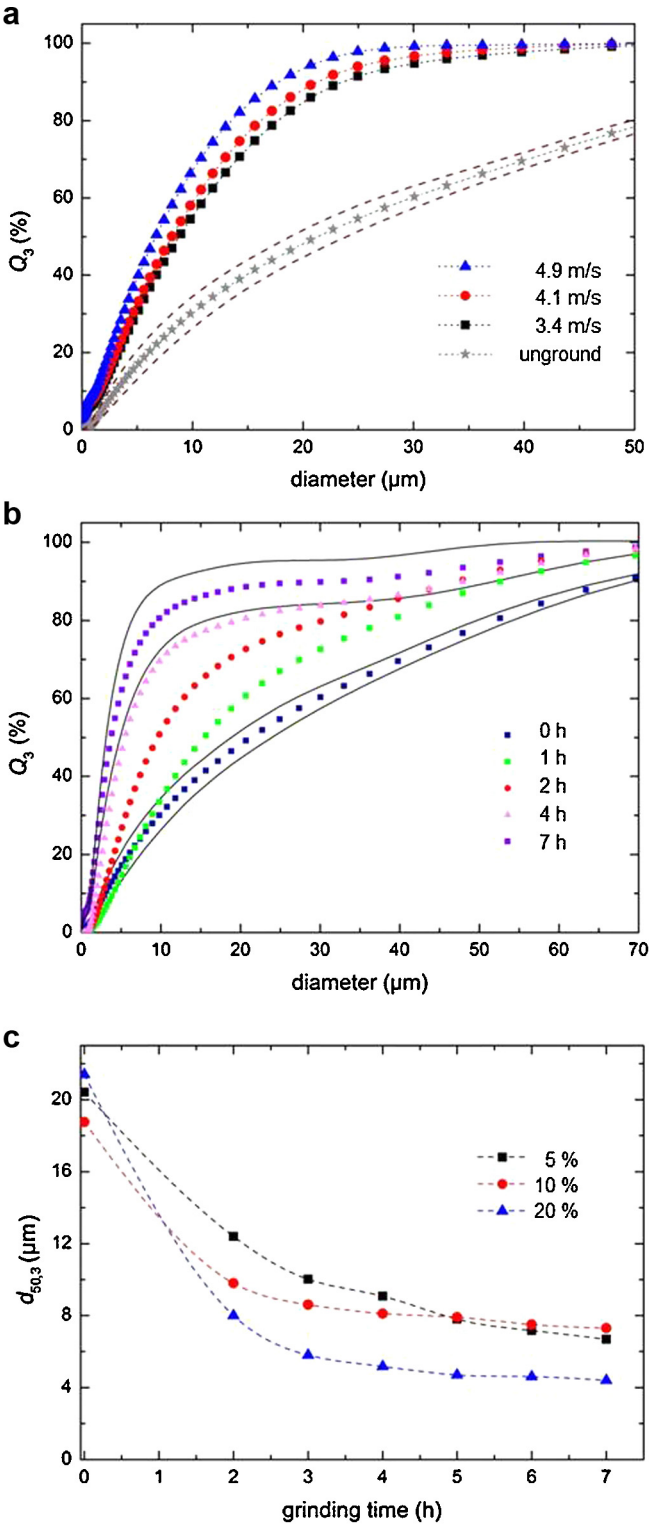


**Fig. 2.** (a) Cumulative particle size distribution of Torlon® 4000 TF poly(amide imide) with a mass concentration of 20% before milling and the distributions after milling with different rotating speeds. The error curves show the standard deviation of the distribution of five different samples before milling (noted unground), each of which was measured three times. (b) Cumulative particle size distribution of Torlon® 4000 TF poly(amide imide) with a mass concentration of 20% for various milling times. The solid lines show the error curves for 0 and 7 h, which were measured 5 and 20 times, respectively. (c) Median volume-related diameter as a function of milling time for three different mass loads.

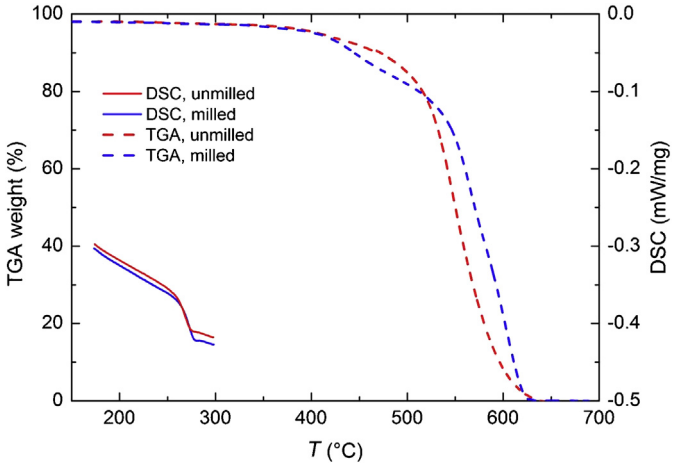


**Fig. 3.** Thermogravimetric analysis curves (dashed lines) and differential scanning calorimetry curves (solid lines) for the as-received polymer powder and after 7 h of milling with 0.5-mm milling balls.

ball abrasion in terms of mass concentration was produced during milling. The remaining mass at $T \sim 700\,^{\circ}C$ was <0.2% both before and after milling. Thus, no significant negative effect of the milling process on the thermal properties of the polymer was observed by TGA and DSC. It is therefore expected that properties that often depend on the thermal behavior of the same polymer (i.e., same polymer type but different chain length), such as strength and ductility, will therefore not be negatively affected by the milling process either. The milling process is assumed to be essentially similar to the milling process for inorganic materials (ceramics and metals), as discussed in detail in the milling literature. However, what is distinctly different from, for example, milled ceramic particles are the minimum particle size limit that can be reached. This limit is determined by the equilibrium between milling and agglomeration for ceramics. For plastically deformable polymers, however, the limit is determined by the size of the plastic zone, as given by Eq. (2).

### 3.4. Minimum particle size

According to Eq. (2), the expected minimum particle size after milling PAI is in the range of $\delta_c \sim 9 - 15\,\mu m$, which is smaller than the value reported by Schmidt et al. (2012) calculated for the polymer PEEK (mainly because of the higher yield stress in PAI) but still larger than the obtained particle size after milling. There are two possible mechanisms that can lead to a smaller particle size after milling than the calculated value: (1) stresses smaller than the calculated values are sufficient for the production of new fracture surfaces, which would be the case when the milling process involves the comminution of agglomerates that are bonded together less strongly, or (2) the primary particles have a slightly spherical shape, as is indicated in Fig. 1. The geometry has an effect on the stress state. A plate-like shape leads to different geometrical factors that enter the calculation of the stress state. The good stability and ease of resuspendability after sedimentation also suggest that the particle size attained is not a consequence of the equilibrium between agglomeration and deagglomeration but that the size reduction may be limited by the stress intensity, which is not sufficiently high to grind the particles to smaller sizes. A further reduction in particle size down to the sub-micrometer range may therefore be feasible if the stress intensity and stress number are increased. It should be noted that mechanochemical effects (Friščić, 2010) may start to become significant in this particle size range, which can have desired or undesired consequences, e.g., in terms of incorporation of nanoparticles abraded from the milling balls

into the polymeric particles or surface modification of the polymer due to the mechanical stress. However, the TGA and DSC analyses (Fig. 3) as well as the relatively large particle sizes (>1 μm) suggest that these effects played at most only a minor role in this study.

## 4. Summary and conclusions

A poly(amide imide) powder with an average particle size $d_{50,3} \sim 22\,\mu m$ was suspended in deionized water and wet-milled using a standard-type attritor. It was observed that poly(amide imide) powder, which is the most important hydrophilic high-performance polymer, could be wet-ground in $H_2O$ to a size as small as $d_{50,3} \sim 3\,\mu m$ using the efficient attritor technique. The suspensions, which had a zeta potential of $\zeta \approx \sim -30\,mV$ and a pH value of 4.5 at a mass concentration of 2% mass, were stable after milling. Several rotor tip speeds, mass concentrations, and ball sizes were tested. Trends similar to those observed for the milling of inorganic materials were obtained in this study, in particular decreasing particle size with increasing number of stress events NS (decreasing ball size). However, a small ball size of 0.5 mm led to stress energies that were too small to grind the largest (>∼20 μm) particles in the suspension such that the $d_{90,3}$ could not be substantially reduced at these ball sizes. No pronounced influence of the rotor tip speed was observed for the tested frequencies (900, 1100, and 1300 rpm). One way to achieve small $d_{50,3}$ and $d_{90,3}$ values simultaneously may be to combine rather small (e.g., 0.5 mm) and large (e.g., 3 mm) ball sizes, which will be investigated in further studies.

## Acknowledgments

We gratefully acknowledge financial support from the German Research Foundation (DFG) via SFB 986 "M$^3$", project A3 and A6, and from the Cluster of Excellence "Integrated Materials Systems" within the Landesexzellenzinitiative Hamburg, Germany.

## References

Becker, G. W., Bottenbruch, L., & Braun, D. (Eds.). (1994). *Kunststoff-handbuch: Band 3/3 Hochleistungskunststoffe*. München Wien: Carl Hanser Verlag.

Blecher, L., Kwade, A., & Schwedes, J. (1996). Motion and stress intensity of grinding beads in a stirred media mill. Part 1. Energy density distribution and motion of single grinding beads. *Powder Technology*, *86*, 59–68.

Breitung-Faes, S., & Kwade, A. (2008). Nano particle production in high-power-density mills. *Chemical Engineering Research & Design*, *86*, 390–394.

Bryce, R. M., Nguyen, H. T., Nakeeran, P., Clement, T., Haugen, C. J., Tykwinski, R. R., et al. (2004). Polyamide-imide polymer thin films for integrated optics. *Thin Solid Films*, *458*, 233–236.

Dugdale, D. S. (1960). Yielding of steel sheets containing slits. *Journal of the Mechanics and Physics of Solids*, *8*, 100–104.

Essl, F., Janssen, R., & Claussen, N. (1999). Wet milling of Al-containing powder mixtures as precursor materials for reaction bonding of alumina (RBAO) and reaction sintering of alumina-aluminide alloys (3A). *Materials Chemistry and Physics*, *61*, 69–77.

Friščić, T. (2010). New opportunities for materials synthesis using mechanochemistry. *Journal of Materials Chemistry*, *20*, 7599–7605.

Knieke, C., Sommer, M., & Peukert, W. (2009). Identifying the apparent and true grinding limit. *Powder Technology*, *195*, 25–30.

Knieke, C., Steinborn, C., Romeis, S., Peukert, W., Breitung-Faes, S., & Kwade, A. (2010). Nanoparticle production with stirred-media mills: Opportunities and limits. *Chemical Engineering & Technology*, *33*, 1401–1411.

Kwade, A. (1999). Wet comminution in stirred media mills—Research and its practical application. *Powder Technology*, *105*, 14–20.

Kwade, A., Blecher, L., & Schwedes, J. (1996). Motion and stress intensity of grinding beads in a stirred media mill. 2. Stress intensity and its effect on comminution. *Powder Technology*, *86*, 69–76.

Kwade, A., & Schwedes, J. (2002). Breaking characteristics of different materials and their effect on stress intensity and stress number in stirred media mills. *Powder Technology*, *122*, 109–121.

Mankosa, M. J., Adel, G. T., & Yoon, R. H. (1986). Effect of media size in stirred ball mill grinding of coal. *Powder Technology*, *49*, 75–82.

Mark, J. E. (Ed.). (1999). *Polymer data handbook*. New York: Oxford University Press, Inc.

Mende, S., Stenger, F., Peukert, W., & Schwedes, J. (2003). Mechanical production and stabilization of submicron particles in stirred media mills. *Powder Technology*, *132*, 64–73.

Munz, D., & Fett, T. (Eds.). (2001). *Ceramics: Mechanical properties, failure behavior, materials selection*. Berlin: Springer.

Nykamp, G., Carstensen, U., & Muller, B. W. (2002). Jet milling—A new technique for microparticle preparation. *International Journal of Pharmaceutics*, *242*, 79–86.

Schmidt, J., Plata, M., Troeger, S., & Peukert, W. (2012). Production of polymer particles below 5 μm by wet grinding. *Powder Technology*, *228*, 84–90.

Sommer, M., Stenger, F., Peukert, W., & Wagner, N. J. (2006). Agglomeration and breakage of nanoparticles in stirred media mills—A comparison of different methods and models. *Chemical Engineering Science*, *61*, 135–148.

Stenger, F., Mende, S., Schwedes, J., & Peukert, W. (2005). Nanomilling in stirred media mills. *Chemical Engineering Science*, *60*, 4557–4565.